JOURNAL OF MATERIALS SCIENCE 16 (1981) 483–488

The kinetics of clustering reactions in iron-doped MgO

T. A. YAGER, W. D. KINGERY
Department of Materials Science and Engineering, Massachusetts Institute of Technology, Cambridge, Massachusetts 02139, USA

Quenched samples of iron-doped MgO crystals have been studied during isothermal annealing treatments using high-temperature EPR spectroscopy. The concentration decay of supersaturated $Fe_{Mg}^{\cdot}$–V_{Mg}'' associates was found to follow second order kinetics. Several different characteristics of the process kinetics are in agreement with our hypothesis that the reaction being observed is the aggregation of two $Fe_{Mg}^{\cdot}$–V_{Mg}'' associates and an unassociated $Fe_{Mg}^{\cdot}$ to form a "3-cluster". Analysis of the decay rate permitted determination of a diffusion coefficient for the associate.

1. Introduction

Trivalent iron enters the MgO lattice substitutionally with its effective positive charge balanced by the negative magnesium vacancy. Using Kröger–Vink notation, the solution process consists of

$$Fe_2O_3 \xrightarrow{MgO} 2Fe_{Mg}^{\cdot} + V_{Mg}'' + 3O_O^x.$$

Coulombic attraction results in formation of $Fe_{Mg}^{\cdot}$–V_{Mg}'' dimers, which may be oriented in either the ⟨1 0 0⟩ (termed D⟨1 0 0⟩) or the ⟨1 1 0⟩ (termed D⟨1 1 0⟩) crystallographic direction [1, 2]. Additional association may occur to form a neutral trimer, consisting of two $Fe_{Mg}^{\cdot}$ associated with one V_{Mg}''. Two linear trimers along the ⟨1 0 0⟩ or ⟨1 1 0⟩ directions and several non-linear trimers may occur.

During the process of phase separation, several intermediate defect clusters may form, as has been found in studies of defect clustering in alkali halide crystals doped with divalent impurities. Following a high temperature quench, Cook and Dryden [3, 4] used dielectric loss measurements periodically during isothermal anneals to monitor the concentration of dimers.* A two-stage third-order kinetic decay was observed, attributed to the aggregation of three dimers to form a cluster, and the growth of higher order complexes. The third-order kinetic decay was subsequently confirmed using electron paramagnetic resonance (EPR) measurements [5] and optical spectroscopy [6]. Based on an analysis of the measured kinetics, the atomistics of defect clustering were evaluated and three mechanisms were proposed for the process [7].

No previous systematic studies of clustering kinetics have been reported for MgO containing trivalent impurities, although the association process at high temperatures has been investigated [1, 2]. The approach used in this study is the application of high-temperature EPR spectroscopy to the evaluation of relaxation phenomena in quenched single crystals of iron-doped MgO.

2. Experimental procedure

A single crystal of 4 N (99.99% pure) MgO doped in the melt with 310 ppm iron was obtained from W. and C. Spicer Ltd., Cheltenham, England. The sample was cleaved along {1 0 0} planes to produce dimensions of 4.8 mm x 4.8 mm x 1 mm. To fully oxidize and homogenize all dopants, the sample was slowly heated to 1600° C in flowing O_2, cooled and held at 1100° C for 24 h, and then quenched into liquid nitrogen.

A high-temperature EPR spectrometer with a CO_2 laser heat source [8] capable of heating to 1200° C and allowing a liquid nitrogen quench within the spectrometer was used to monitor defect concentrations. In the spectrometer the

---

*The literature on alkali halide systems refers to what we call dimers as "dipoles".

0022–2461/81/020483–06$02.60/0

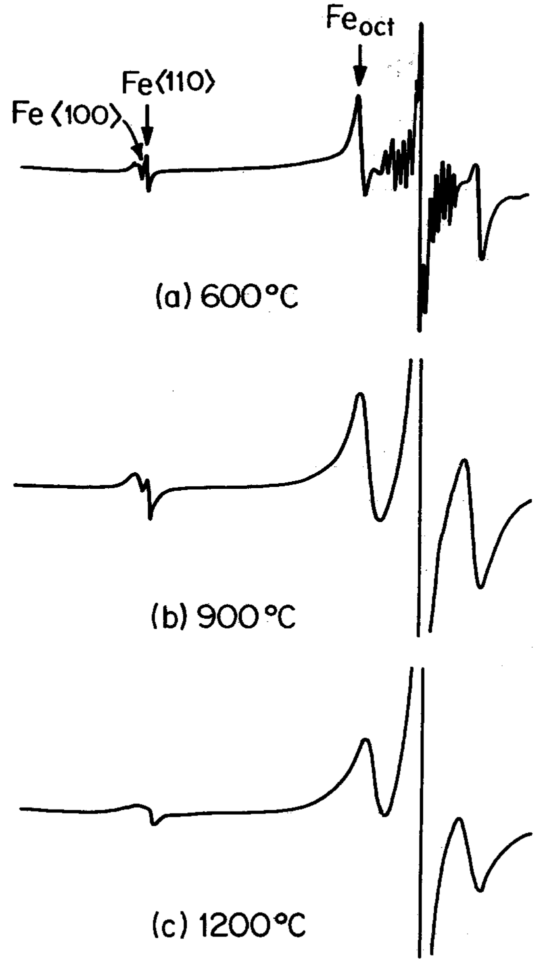

Figure 1 EPR spectra of MgO containing 310 ppm Fe during an isothermal anneal at 500° C.

sample was first heated to 1200° C for 15 min, lowered to 1100° C for 30 min, and then quenched. The sample was then heated to 400° C within a few seconds for an isothermal anneal. During the anneal the EPR spectra were recorded at appropriate time intervals. When a spectrum decayed to less than half of its initial intensity, the sample was rapidly heated to 1200° C for 15 min, and the same procedure was repeated for isothermal anneals at 425, 450, 475 and 500° C. Isothermal anneals were also conducted at 500, 525, 550, 575 and 600° C; at these temperatures sufficient time was allowed for decay to a constant value.

3. Results and discussion

3.1. The spectra

EPR spectra of MgO containing 310 ppm Fe during a 500° C isothermal anneal are shown in Fig. 1 at three different times. Peaks have been labelled Fe⟨1 0 0⟩, Fe⟨1 1 0⟩, and $\mathrm{Fe_{oct}}$, attributed to $\mathrm{Fe}^{\bullet}_{\mathrm{Mg}}$–$\mathrm{V}''_{\mathrm{Mg}}$ associates oriented in the ⟨1 0 0⟩ direction [9], the ⟨1 1 0⟩ direction [10] and an unassociated $\mathrm{Fe}^{\bullet}_{\mathrm{Mg}}$ [11]. The $\mathrm{Fe_{oct}}$ peak is the low magnetic field part of a well-known quintet of peaks attributed to ferric iron in an octahedral site [11]. Rotation of the magnetic field around the crystal identified the Fe⟨1 0 0⟩ and Fe⟨1 1 0⟩ spectral peaks as due to tetragonal [9] and orthorhombic [10] defect centres. Changes in the equilibrium concentration of the Fe⟨1 1 0⟩ centre has provided evidence indicating that it is predominantly a dimer [12].

The double integrated EPR signal intensity is proportional to the concentration of its defect centre. In the absence of broadening effects the peak-to-peak signal intensity can be used to measure relative concentration. Thus $I_i = a_i X_i$, where I_i is the peak-to-peak signal intensity, X_i is the concentration of the defect giving rise to the resonance, and a_i is a proportionality factor dependent on the oscillator strength of the transition, sample size, temperature, peak shape and the instrumental gain of the spectrometer. In the following analysis, a_i is assumed to be a constant at a specific temperature.

3.2. The decay of the EPR spectra

The Fe⟨1 1 0⟩ peak has provided the most information about the kinetic reactions. Since only one vacancy jump transforms a D⟨1 1 0⟩ dimer to a D⟨1 0 0⟩ orientation, their concentrations are assumed to be in metastable equilibrium and proportional to each other. Therefore, the signal intensity of the Fe⟨1 1 0⟩ peak serves to measure not only the concentration of the dimer oriented in the ⟨1 1 0⟩ direction, but (with a different proportionality constant) the total dimer concentration as well, i.e.

$$\begin{aligned} I_{\mathrm{Fe}\langle 110\rangle} &= a_{\mathrm{Fe}\langle 110\rangle}[\mathrm{D}\langle 1\,1\,0\rangle] \\ &= a_{\mathrm{Fe}\langle 110,\,100\rangle}([\mathrm{D}\langle 1\,1\,0\rangle] + [\mathrm{D}\langle 1\,0\,0\rangle]) \\ &= a_{\mathrm{Fe}\langle 110,\,100\rangle}[\mathrm{D}\langle 1\,0\,0,\,1\,1\,0\rangle], \end{aligned}$$

where the notation ⟨1 1 0, 1 0 0⟩ implies a contribution of both the ⟨1 1 0⟩ and ⟨1 0 0⟩ species. Experimentally it was found that the Fe⟨1 0 0⟩ peak followed the same decay kinetics as the Fe⟨1 1 0⟩ peak.

During the isothermal anneals, Fe⟨1 1 0⟩ was analysed for the order of kinetic decay. The data did not fit either first- or third-order decay, but a

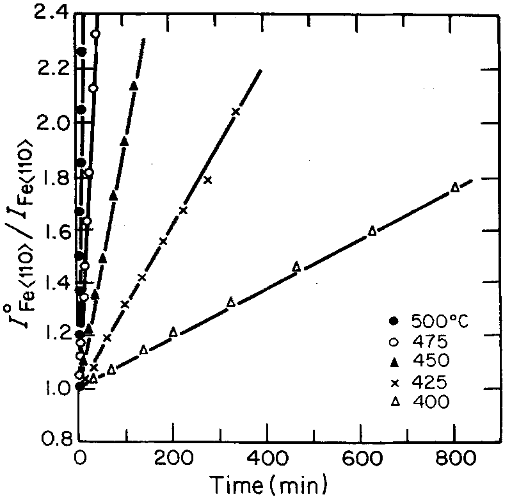

Figure 2 Second-order plot for Fe⟨1 1 0⟩ decay during isothermal anneal of MgO containing 310 ppm Fe.

plot of $1/I_{\mathrm{Fe}\langle 1\,1\,0\rangle}$ against time for the temperature range 400 to 500° C is linear, indicating a second-order reaction, i.e.

$$\frac{\mathrm{d}c}{\mathrm{d}t} = -kc^2.$$

Integrating, $1/c = kt + 1/c_0$ and letting $c = [\mathrm{D}\langle 1\,1\,0, 1\,0\,0\rangle] = I_{\mathrm{Fe}\langle 1\,1\,0\rangle}/a_{\mathrm{Fe}\langle 1\,1\,0, 1\,0\,0\rangle}$,

$$1/I_{\mathrm{Fe}\langle 1\,1\,0\rangle} = \frac{kt}{a_{\mathrm{Fe}\langle 1\,1\,0,\,1\,0\,0\rangle}} + \frac{1}{I^0_{\mathrm{Fe}\langle 1\,1\,0\rangle}},$$

where $I^0_{\mathrm{Fe}\langle 1\,1\,0\rangle}$ is the initial value at time zero. A plot of $1/I_{\mathrm{Fe}\langle 1\,1\,0\rangle}$ against time for each temperature gave an intercept of $1/I^0_{\mathrm{Fe}\langle 1\,1\,0\rangle}$. A form independent of the unknown value of $a_{\mathrm{Fe}\langle 1\,1\,0,\,1\,0\,0\rangle}$ is obtained by dividing each intensity by its appropriate linear intercept. Then,

$$I^0_{\mathrm{Fe}\langle 1\,1\,0\rangle}/I_{\mathrm{Fe}\langle 1\,1\,0\rangle} = k[\mathrm{D}^0\langle 1\,1\,0, 1\,0\,0\rangle]t + 1, \quad (1)$$

which is plotted in Fig. 2, confirming the second-order decay.

The intensity of the $\mathrm{Fe_{oct}}$ peak was found to decay at a rate proportional to the decay of the Fe⟨1 1 0⟩ peak. Therefore,

$$\frac{\mathrm{d}[\mathrm{Fe_{oct}}]}{\mathrm{d}t} = B\frac{\mathrm{d}[\mathrm{D}\langle 1\,1\,0, 1\,0\,0\rangle]}{\mathrm{d}t}$$

$$= -kB[\mathrm{D}\langle 1\,1\,0, 1\,0\,0\rangle]^2, \quad (2)$$

where B is a constant. Solving Equation 1 for $[\mathrm{D}\langle 1\,1\,0, 1\,0\,0\rangle]$ and integrating Equation 2,

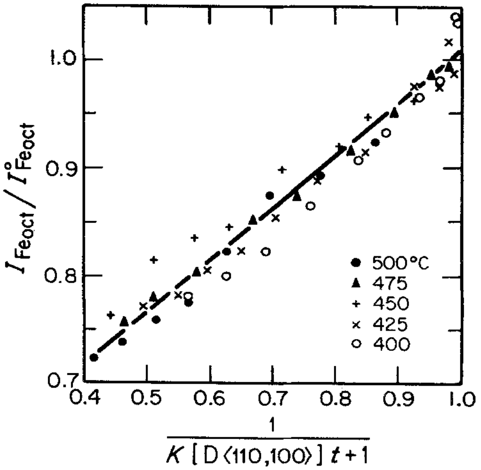

Figure 3 Kinetic decay of $\mathrm{Fe_{oct}}$ during isothermal anneal of MgO containing 310 ppm Fe.

$$[\mathrm{Fe_{oct}}] = -kB\int\frac{\mathrm{d}t}{(kt + 1/[\mathrm{D}^0\langle 1\,1\,0, 1\,0\,0\rangle])^2}$$

$$= B[\mathrm{D}^0\langle 1\,1\,0, 1\,0\,0\rangle] \times \left(\frac{1}{k[\mathrm{D}^0\langle 1\,1\,0, 1\,0\,0\rangle]t + 1}\right) + ([\mathrm{Fe^0_{oct}}] - B[\mathrm{D}^0\langle 1\,1\,0, 1\,0\,0\rangle])$$

to give

$$I_{\mathrm{Fe_{oct}}} = a_{\mathrm{Fe_{oct}}}B[\mathrm{D}^0\langle 1\,1\,0, 1\,0\,0\rangle] \times \left(\frac{1}{k[\mathrm{D}^0\langle 1\,1\,0, 1\,0\,0\rangle]t + 1}\right) + (I^0_{\mathrm{Fe_{oct}}} - a_{\mathrm{Fe_{oct}}}B[\mathrm{D}^0\langle 1\,1\,0, 1\,0\,0\rangle]).$$

A plot of $I_{\mathrm{Fe_{oct}}}$ against $1/(k[\mathrm{D}^0\langle 1\,1\,0, 1\,0\,0\rangle]t + 1)$ provided a slope of $a_{\mathrm{Fe_{oct}}}B[\mathrm{D}^0\langle 1\,1\,0, 1\,0\,0\rangle]$ and an intercept of $(I^0_{\mathrm{Fe_{oct}}} - a_{\mathrm{Fe_{oct}}}B[\mathrm{D}^0\langle 1\,1\,0, 1\,0\,0\rangle])$. A normalized plot was obtained for each temperature by dividing each $I_{\mathrm{Fe_{oct}}}$ by the appropriate slope minus the intercept to yield

$$\frac{[\mathrm{Fe_{oct}}]}{[\mathrm{Fe^0_{oct}}]} = \frac{I_{\mathrm{Fe_{oct}}}}{I^0_{\mathrm{Fe_{oct}}}} = \frac{B[\mathrm{D}^0\langle 1\,1\,0, 1\,0\,0\rangle]}{[\mathrm{Fe^0_{oct}}]} \times \left(\frac{1}{k[\mathrm{D}^0\langle 1\,1\,0, 1\,0\,0\rangle]t + 1}\right) + \left(1 - \frac{B[\mathrm{D}^0\langle 1\,1\,0, 1\,0\,0\rangle]}{[\mathrm{Fe^0_{oct}}]}\right).$$

This is plotted in Fig. 3, from which a new slope and intercept were obtained. The linear least-squares best fit of the experimental data yielded

$$\frac{I_{\mathrm{Fe_{oct}}}}{I^0_{\mathrm{Fe_{oct}}}} = 0.48\left(\frac{1}{k[\mathrm{D^0}\langle 1\,1\,0, 1\,0\,0\rangle]\,t+1}\right)+0.52. \tag{3}$$

3.3. The 3-cluster

The second-order decay of dimers implies the reaction of two dimers to form an initial cluster. Electrostatic repulsion of the negatively charged dimers makes a direct combination unlikely and suggests that a positively charged defect might be involved. Consider

$$2\ \text{dimers} + \mathrm{Fe}^{\bullet}_{\mathrm{Mg}} = \text{3-cluster}. \tag{4}$$

Since direct reaction would involve a three-body collision, a two-step process seems more likely, i.e.

$$\text{dimer} + \mathrm{Fe}^{\bullet}_{\mathrm{Mg}} = \text{trimer}; \tag{5}$$

$$\text{dimer} + \text{trimer} = \text{3-cluster}. \tag{6}$$

As has been discussed in some detail by Reiss *et al.* [13], this two-step process leads to second-order kinetics so long as the first step is slower and the $\mathrm{Fe}^{\bullet}_{\mathrm{Mg}}$ and trimer species act as immobile traps for the mobile dimers. Similar kinetics are found for impurity pairing reactions in germanium [13]. Equation 5 would be expected to be the slower process based on electrostatic and structural constraints similar to those suggested to occur in the alkali halide systems by Strutt and Lilley [7].

According to Equation 4, the value of B in Equation 2 should equal 0.5. From Equation 3 the experimentally determined parameters indicate that

$$\frac{B[\mathrm{D^0}\langle 1\,1\,0, 1\,0\,0\rangle]}{[\mathrm{Fe^0_{oct}}]} = 0.48 \simeq 0.5$$

or $[\mathrm{D^0}\langle 1\,1\,0, 1\,0\,0\rangle] \simeq [\mathrm{Fe^0_{oct}}]$. Thus, following the quench the concentration of dimers approximately equals the concentration of unassociated iron, which implies that very few vacancies remain unassociated, a result in accord with several EPR studies [14].

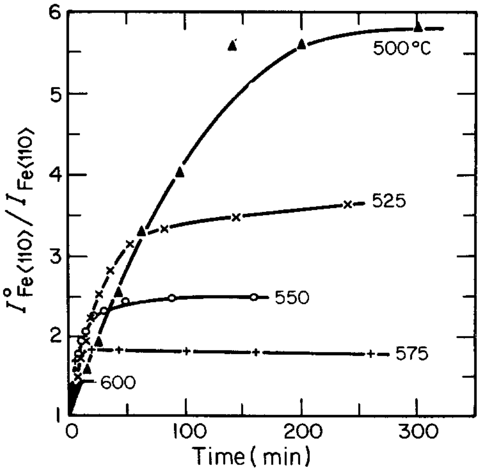

Figure 4 Normalized second order decay plot for Fe⟨1 1 0⟩ during isothermal anneal of MgO containing 310 ppm Fe.

The kinetic behaviour of the Fe⟨1 1 0⟩ peak during long isothermal anneals from 500 to 600° C was used to evaluate the metastable equilibrium properties of the 3-cluster. A normalized second-order decay plot, using Equation 1, is shown in Fig. 4 for isothermal anneals at 500, 525, 550, 575 and 600° C. The second-order decay eventually levelled off, indicating a metastable equilibrium. From Equation 4 the equilibrium constant for the formation of the 3-cluster can be written

$$\frac{[\text{3-cluster}]_{\mathrm{eq}}}{[\text{dimer}]^2_{\mathrm{eq}}\,[\mathrm{Fe}^{\bullet}_{\mathrm{Mg}}]_{\mathrm{eq}}} = K_{0,\text{3-cluster}} \exp\left(\frac{E_{\text{3-cluster}}}{kT}\right). \tag{7}$$

Letting $[\mathrm{Fe}^{\bullet}_{\mathrm{Mg}}]_{\mathrm{eq}} = [\mathrm{D^0}\langle 1\,1\,0,\ 1\,0\,0\rangle] - 1/2([\mathrm{D^0}\langle 1\,1\,0, 1\,0\,0\rangle] - [\mathrm{D}\langle 1\,1\,0, 1\,0\,0\rangle]_{\mathrm{eq}})$ and $[\text{3-cluster}]_{\mathrm{eq}} = 1/2([\mathrm{D^0}\langle 1\,1\,0,\ 1\,0\,0\rangle] - [\mathrm{D}\langle 1\,1\,0, 1\,0\,0\rangle]_{\mathrm{eq}})$, with a manipulation of terms

$$\ln\left\{\frac{1-\left(\dfrac{I^{\mathrm{eq}}_{\mathrm{Fe}\langle 1\,1\,0\rangle}}{I^0_{\mathrm{Fe}\langle 1\,1\,0\rangle}}\right)}{\left(\dfrac{I^{\mathrm{eq}}_{\mathrm{Fe}\langle 1\,1\,0\rangle}}{I^0_{\mathrm{Fe}\langle 1\,1\,0\rangle}}\right)^2\left(1+\left[\dfrac{I^{\mathrm{eq}}_{\mathrm{Fe}\langle 1\,1\,0\rangle}}{I^0_{\mathrm{Fe}\langle 1\,1\,0\rangle}}\right]\right)}\right\} = \frac{E_{\text{3-cluster}}}{kT} + \ln\,[\mathrm{D^0}\langle 1\,1\,0, 1\,0\,0\rangle]K_{0,\text{3-cluster}}. \tag{8}$$

A plot of Equation 8 is shown in Fig. 5. A straight line resulted, yielding a least-squares fit of

$$\ln\left\{\frac{1-\left(\dfrac{I^{\mathrm{eq}}_{\mathrm{Fe}\langle 1\,1\,0\rangle}}{I^0_{\mathrm{Fe}\langle 1\,1\,0\rangle}}\right)}{\left(\dfrac{I^{\mathrm{eq}}_{\mathrm{Fe}\langle 1\,1\,0\rangle}}{I^0_{\mathrm{Fe}\langle 1\,1\,0\rangle}}\right)^2\left(1+\left[\dfrac{I^{\mathrm{eq}}_{\mathrm{Fe}\langle 1\,1\,0\rangle}}{I^0_{\mathrm{Fe}\langle 1\,1\,0\rangle}}\right]\right)}\right\} = \frac{2.76\times 10^4}{T} - 32.61.$$

The equilibrium constant for Equation 7 is thus

$$K_{\text{3-cluster}} = \frac{6.9\times 10^{-15}}{[\mathrm{D^0}\langle 1\,1\,0, 1\,0\,0\rangle]^2} \exp\frac{2.4\,\mathrm{eV}}{kT}.$$

The value of $K_{0,\text{3-cluster}}$ was approximated by assuming $[\mathrm{D^0}\langle 1\,1\,0, 1\,0\,0\rangle] \simeq 30$ ppm (one-tenth

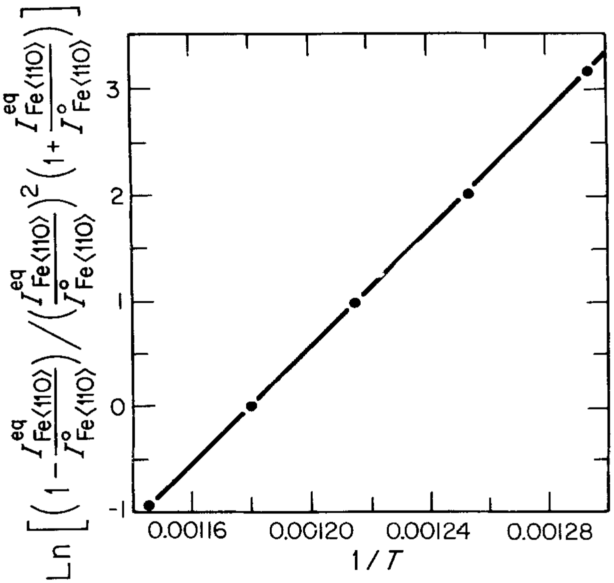

Figure 5 Formation of the 3-cluster during isothermal anneal of MgO containing 310 ppm Fe.

the total iron concentration), then

$$K_{3\text{-cluster}} \simeq 8 \times 10^{-6} \exp \frac{2.4\,\text{eV}}{kT}. \qquad (9)$$

The dependence of $K_{0,3\text{-cluster}}$ on an estimation of $[\mathrm{D^0}\langle 1\,1\,0, 1\,0\,0\rangle]$ limits it to being a first-order approximation. The exponential could vary within ± 0.1 eV, based on the ± 10° C error in the absolute temperature, but, in addition, the calculation is based on the assumption that $[\mathrm{D^0}\langle 1\,1\,0, 1\,0\,0\rangle]$ is equivalent at all temperatures between 500 and 600° C. A worst-case analysis indicated that $E_{3\text{-cluster}}$ should be within the limits of 2.3 to 2.8 ± 0.1 eV [15].

3.4. Diffusion of the dimer

The decay rate of the Fe⟨1 1 0⟩ peak was also used to analyse the diffusional properties of the dimer. For a diffusion-limited reaction, the kinetic decay constant can be written

$$k \simeq \frac{k_0}{T} \exp \frac{-Q}{kT},$$

where k_0 is a constant dependent on the initial concentration of all reacting species, and Q represents the activation energy barrier for the diffusion of the rate-limiting species. Fig. 6 shows a plot of $\ln(k[\mathrm{D^0}\langle 1\,1\,0, 1\,0\,0\rangle]T)$ against $1/T$, where $k[\mathrm{D^0}\langle 1\,1\,0, 1\,0\,0\rangle]$ was obtained from the slope at each temperature in Fig. 2. A straight line resulted, as expected for a diffusion limited reaction, and linear regression yielded

$$k[\mathrm{D^0}\langle 1\,1\,0, 1\,0\,0\rangle]T = 1.6 \times 10^{15} \exp \frac{-2.1\,\text{eV}}{kT}. \qquad (10)$$

The pre-exponential for dimer diffusion was approximated using the analysis derived by Reiss *et al.* for a similar experiment [13]. With the following boundary conditions

$$[\mathrm{D^0}\langle 1\,1\,0, 1\,0\,0\rangle] = [\mathrm{Fe^{\cdot}_{Mg}}],$$

$$\zeta(\infty) = 2[\mathrm{D^0}\langle 1\,1\,0, 1\,0\,0\rangle],$$

$$\zeta(R) = 0,$$

and $$\zeta(r) = 2[\mathrm{D^0}\langle 1\,1\,0, 1\,0\,0\rangle]^2(1 - R/r),$$

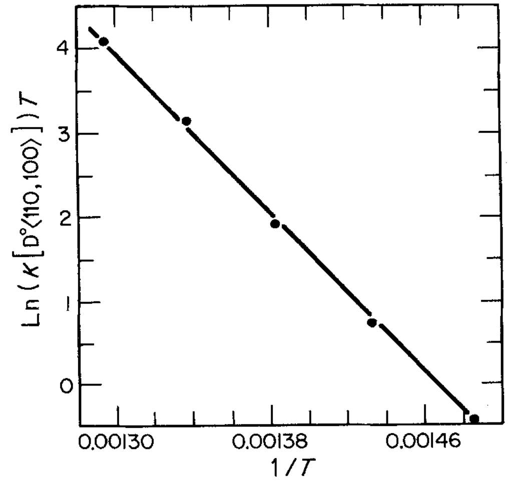

Figure 6 Activation energy for clustering of Fe⟨1 1 0⟩ during isothermal anneal of MgO containing 310 ppm Fe.

the rate constant for dimer decay can be expressed as

$$k = \frac{8\pi e^2 D_0}{K_s k_b T} \exp \frac{-Q}{k_b T}, \qquad (11)$$

where ζ, R, r, K_s, k_b and D_0 are the density of dimers around an isolated iron, the effective capture radius, the distance between an isolated $\text{Fe}^{\bullet}_{\text{Mg}}$ and a dimer, the static dielectric constant, Boltzmann's constant, and the pre-exponential for dimer diffusion, respectively. From Equations 10 and 11

$$k_0[\text{D}^0\langle 1\,1\,0, 1\,0\,0\rangle] = \frac{8\pi e^2 D_0 [\text{D}^0\langle 1\,1\,0, 1\,0\,0\rangle]}{k_b K_s}$$

$$= 1.6 \times 10^{15}\,\text{K}\,\text{sec}^{-1}$$

or

$$D_{\text{dimer}} = \frac{3.9 \times 10^{17}}{[\text{D}^0\langle 1\,1\,0, 1\,0\,0\rangle]} \exp \frac{-Q}{k_b T} (\text{cm sec})^{-1}.$$

Approximating $[\text{D}^0\langle 1\,1\,0, 1\,0\,0\rangle] \simeq 30\,\text{ppm}$ $(1.6 \times 10^{18}\,\text{cm}^{-3})$,

$$D_{\text{dimer}} \simeq 0.2 \exp \frac{-2.1\,\text{eV}}{k_b T}\,\text{cm}^2\,\text{sec}^{-1}. \qquad (12)$$

The pre-exponential may vary from 0.1 to $1.0\,\text{cm}^2\,\text{sec}^{-1}$ depending on the estimate of $[\text{D}^0\langle 1\,1\,0, 1\,0\,0\rangle]$. A worst-case analysis set limits on the exponential of $-2.1 \pm 0.2\,\text{eV}$ [15].

4. Summary

In low dopant level crystals of iron-doped MgO quenched from 1100° C into liquid nitrogen, the second-order concentration decay of $\text{Fe}^{\bullet}_{\text{Mg}}\text{–V}''_{\text{Mg}}$ dimers is in accord with a process consisting of aggregation of two dimers and an unassociated iron to form a 3-cluster similar to reactions found in alkali halides doped with divalent cations. Interpretation of reaction kinetics according to this model permitted evaluation of the dimer diffusion coefficient and the equilibrium constant for 3-cluster formation. Relaxation during the quench was found to deplete the system of unassociated vacancies, leaving a room-temperature supersaturation of unassociated $\text{Fe}^{\bullet}_{\text{Mg}}$ and dimers in equal concentrations.

Acknowledgement

This research was conducted at the Massachusetts Institute of Technology with the support of the US Department of Energy under Contract No. EY-76-S-02-2390.

References

1. W. H. GOURDIN and W. D. KINGERY, *J. Mater. Sci.* **14** (1979) 2053.
2. W. H. GOURDIN, W. D. KINGERY and J. DRIEAR, *ibid.* **14** (1979) 2074.
3. J. S. COOK and J. S. DRYDEN, *Aust. J. Phys.* **13** (1960) 260.
4. *Idem, Proc. Phys. Soc.* **80** (1962) 479.
5. H. F. SYMMONS and R. C. KEMP, *Brit. J. Appl. Phys.* **17** (1966) 607.
6. J. S. DRYDEN and G. G. HARVEY, *J. Phys. C.* **2** (1969) 603.
7. J. E. STRUTT and E. LILLEY, *Phys. Stat. Sol. (a)* **33** (1976) 229.
8. T. A. YAGER and W. D. KINGERY, *Rev. Sci. Instrum.* **51** (1980) 464.
9. B. HENDERSON, J. E. WERTZ, T. P. P. HALL and R. D. DOWSING, *J. Phys. C.* **4** (1971) 107.
10. R. S. DE BIASI and A. CALDAS, *ibid.* **10** (1977) 107.
11. W. LOW, *Proc. Phys. Soc. London* **B69** (1956) 1169.
12. T. A. YAGER and W. D. KINGERY, *J. Mater. Sci.* **16** (1981) 489.
13. H. REISS, C. S. FULLER and F. J. MORIN, *Bell Sys. Tech. J.* **35** (1956) 535, 582.
14. Y. CHEN, M. M. ABRAHAM, L. C. TEMPLETON and W. P. UNRUH, *Phys. Rev. B* **11** (1975) 881.
15. T. A. YAGER, Ph.D. Thesis, MIT, 1980.

Received 29 May and accepted 28 July 1980.